

Dielectric nonlinearity of PVDF–TrFE copolymer

B. Ploss*, B. Ploss

Department of Applied Physics and Materials Research Centre, The Hong Kong Polytechnic University, Hung Hom, Kowloon, Hong Kong, People's Republic of China

Received 2 August 1999; received in revised form 25 October 1999; accepted 11 November 1999

Abstract

The experimental study of small signal dielectric nonlinearity is a powerful procedure for the investigation of complex ferroelectric materials. Dielectric nonlinearity of a copolymer of polyvinylidene fluoride with trifluoroethylene, in the compositions 70/30 and 56/44 mol%, has been measured by an analysis of the harmonic spectrum of the electric current in response to a sinusoidal voltage. The Landau parameters of the crystalline phase are determined from the experimental data, and the order of the phase transition is discussed. It is found that the values of the Landau parameter γ in the ferroelectric and in the paraelectric phase are different. In the ferroelectric phase γ is a function of the degree of poling. The experimental results are also compared with theoretical predictions derived from Odajima's microscopic model, which assumes a one-dimensional Ising model for the dipolar coupling along the polymer chains and a mean field theory for the interchain interaction. Copolymer film deposited from a solution that is poled before annealing shows a small second-order dielectric nonlinearity even in the paraelectric phase. The reason for this is a non-switchable polarization, which is stable above the Curie temperature. We attribute this polarization to the intermediate phase in between the crystallites and the amorphous regions. © 2000 Elsevier Science Ltd. All rights reserved.

Keywords: Poly(VDF–TrFE); Nonlinear dielectricity; Ferroelectric transitions

1. Introduction

The investigation of nonlinear dielectric permittivities gives valuable information on the ferroelectric properties of a material. The permittivities of odd order give direct access to the free energy (Landau parameters) [1–3] and the order of the phase transition [4,5]. The second-order permittivity provides information on the degree of poling [6] and the existence of fixed dipoles [7]. The method should, in particular, be suitable for describing complicated ferroelectric systems such as the semicrystalline polyvinylidene fluoride–trifluoroethylene, P(VDF–TrFE), copolymers, as it provides much more information than the linear permittivity alone. P(VDF–TrFE) copolymers consist of ferroelectric regions with crystalline order embedded in an amorphous matrix. They exhibit a diffuse phase transition from the ferroelectric to the paraelectric phase caused by a statistical variation of the VDF content of the crystallites [8]. The dielectric properties of the copolymers near the phase transition depend strongly on the composition of VDF and TrFE.

In this work the nonlinear dielectric properties of P(VDF–TrFE) copolymers are investigated and some interesting conclusions are obtained from the results. The data are compared with a detailed phenomenological description. A microscopical approach developed by Odajima [9] for describing the polarization of P(VDF–TrFE) copolymers is, for the first time, considered with respect to the nonlinear dielectric permittivities and compared with the experimental results.

2. Theory

2.1. Model for the nonlinear dielectric properties of a semicrystalline ferroelectric system

Fig. 1 illustrates the structure of a semicrystalline polymer (Fig. 1a) and its approximation by a brick like structure (Fig. 1b) as proposed for PVDF [10]. For this structure, the electric field in the whole sample is assumed to be in parallel to the external field, and the dielectric properties are described by a capacitor model (Fig. 1c). The ferroelectric crystalline system is characterized by nonlinear dielectric permittivities ϵ_{cn} defined by the expansion of the dielectric displacement D in powers of

* Corresponding author. Tel.: + 852-2766-5679; fax: + 852-2333-7629.

E-mail address: apploss@polyu.edu.hk (B. Ploss).

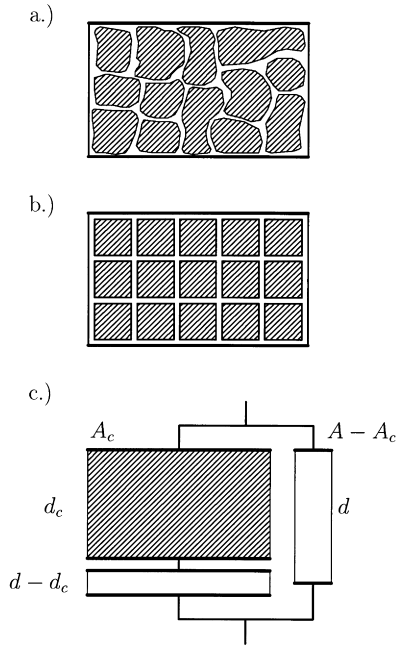


Fig. 1. Model for the dielectric properties of the semicrystalline copolymers: (a) ferroelectric crystallites embedded in an amorphous matrix; (b) simplification of the geometry; and (c) capacitor model. A , A_c , d and d_c are the electrode areas and thickness of the capacitors representing the entire specimen and the crystalline system, respectively.

the electric field E :

$$D = P_{cs} + \varepsilon_0 \varepsilon_{c1} E + \varepsilon_0 \varepsilon_{c2} E^2 + \varepsilon_0 \varepsilon_{c3} E^3 + \dots \quad (1)$$

The amorphous system is described by the linear permittivity ε_a . The calculation of the effective nonlinear dielectric permittivities ε_n of the whole system yields [11]:

$$\varepsilon_1 = \frac{X_c}{h} \frac{\varepsilon_{c1}}{h + (1-h)\varepsilon_{c1}/\varepsilon_a} + \left(1 - \frac{X_c}{h}\right) \varepsilon_a, \quad (2)$$

$$\varepsilon_n = X_c \frac{\varepsilon_{cn}}{(h + (1-h)\varepsilon_{c1}/\varepsilon_a)^{n+1}}, \quad \text{for } n > 1. \quad (3)$$

where $X_c = V_c/V$ is the volume fraction of the crystalline part, i.e. the crystallinity of the sample. The quotient $h = d_c/d$ of the thickness of the crystalline region and the sample depends on the shape of the crystallites. For cubic crystallites, h is equal to $\sqrt[3]{X_c}$.

2.2. Phenomenological theory for the crystalline system

Ferroelectrics near the phase transition are usually described phenomenologically by the Landau free energy

$$F = F_0 + \frac{1}{2} \alpha D^2 + \frac{1}{4} \gamma D^4 + \frac{1}{6} \delta D^6. \quad (4)$$

Using the nonlinear relation between the electric field $E = \partial F / \partial D$ and the dielectric displacement, the nonlinear dielectric permittivities ε_{cn} can be calculated as a function of the Landau parameters α , γ and δ . In the paraelectric phase $P_s = 0$ and the permittivities of even order vanish. The

permittivities of the odd order are

$$\varepsilon_0 \varepsilon_{c1} = 1/\alpha \quad \varepsilon_0 \varepsilon_{c3} = -\gamma/\alpha^4 \quad \varepsilon_0 \varepsilon_{c5} = (3\gamma^2 - \alpha\delta)/\alpha^7. \quad (5)$$

A measurement of the odd-order permittivities of a crystalline ferroelectric gives direct access to the temperature dependencies of the Landau parameters α , γ and δ in the paraelectric phase. In particular, the sign of the third-order permittivity in the paraelectric phase yields the sign of γ , which according to the Landau theory determines the order of the phase transition [4].

In the ferroelectric phase, the second-order permittivity of the crystalline system is given by [6]:

$$\varepsilon_0 \varepsilon_{c2} = -P_{cr}(\varepsilon_0 \varepsilon_1)^3 (3\gamma + 10\delta P_s^2) \quad (6)$$

with the mean polarization of the crystalline system $P_{cr} = X_p P_s$. The factor X_p is the degree of polarization and is equal to one if all dipoles are oriented in parallel to the poling field. For copolymer material with randomly oriented crystallite axes, fully poled samples would have a polarization degree of $X_p \approx 2/3$ [12].

2.3. Microscopical theory for the crystalline system

P(VDF-TrFE) copolymers with a VDF content above 60 mol% show thermal hysteresis, i.e. the phase transition is of first-order, while for copolymers with lower VDF content no thermal hysteresis is observed. Odajima [9] derived a microscopical theory which is capable of describing both the first and the second-order phase transitions depending on the intrachain interaction energy J . The interaction of the dipoles along one polymer chain is described by a one-dimensional Ising model, while the dipolar interaction with the z neighbored chains is taken into account by a mean field approximation with the interchain interaction energy L . An approximation in the theory is the use of the same mean dipole moment μ for the VDF and TrFE monomers with the dipole density N . Furthermore, *trans* and *gauche* bondings are simplified by parallel and antiparallel orientations of the dipoles, respectively. The interaction energy is equal to the energy difference between the *trans* and *gauche* bondings $J = u_G - u_T$. As a result, Odajima obtains a relation between P and E :

$$\frac{P}{N\mu} = \frac{e^{J/kT} \sinh(\mu E + zLP/2N\mu)/kT}{\sqrt{1 + e^{2J/kT} \sinh^2(\mu E + zLP/2N\mu)/kT}} \quad (7)$$

The spontaneous polarization P_s is given by the zeros of $E(P)$ with a positive derivation dE/dP . For comparison with the experimental data we have derived the nonlinear dielectric permittivities from Eq. (7) using a recursion procedure. For comparing the microscopical and the phenomenological theories, the Landau parameters can be evaluated by a power series expansion of $E(P)$. The expression of α shows that the Curie temperature T_0 and the interchain interaction energy $zL = 2kT_0 e^{-J/kT_0}$ are directly

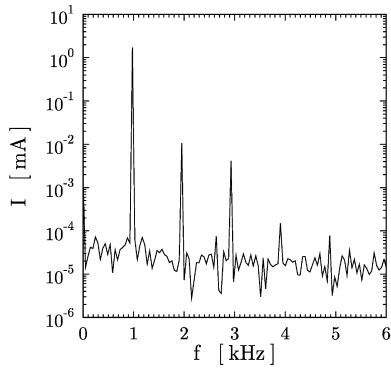


Fig. 2. Fourier spectrum of the current through a poled 56/44 mol% VDF–TrFE copolymer sample during application of a sinusoidal electric field with frequency 977 Hz and amplitude 7 V/μm.

related. γ is positive for $J > -kT \ln 3/2$ and negative for $J < -kT \ln 3/2$. δ is always positive.

3. Measurement principle

In order to measure the nonlinear dielectric permittivities ϵ_n , a sinusoidal electrical field with the frequency $f_0 = 1$ kHz ($\omega_0 = 2\pi f_0$) and an amplitude E_{\sim} far below the coercive field is applied to the sample. A signal with high spectral purity is generated by appropriate filtering of the output

signal of a frequency synthesizer. The current through the sample is recorded by the voltage over a series resistor and digitized by a 16 bit A–D converter at a sampling period of 20 μs. Spectra of the current density $j(t)$ are calculated by Fourier transform:

$$j(t) = \frac{d}{dt}D(t) = \sum_{l=0}^{\infty} (j'_l \cos l\omega_0 t + j''_l \sin l\omega_0 t) \quad (8)$$

Fig. 2 shows as an example the Fourier spectrum of the current through a poled 56/44 mol% VDF–TrFE copolymer. The nonlinear permittivities ϵ_n can be evaluated from a sum of Fourier coefficients j''_l [2]. If the excitation amplitude is chosen appropriately, i.e. sufficiently small so that the coefficients j''_n decrease strongly with increasing order n , then ϵ_n can be approximately calculated from the component j''_n .

$$\epsilon_0 \epsilon_n \approx \frac{-1}{\omega_0} \frac{2^{n-1}}{n E_{\sim}^n} j''_n. \quad (9)$$

In the general case, the ϵ_n defined by Eq. (9) form the real parts ϵ'_n of the complex nonlinear permittivities. Non-vanishing components j'_n can be described by the definition of imaginary parts ϵ''_n that are calculated from j'_n analogous to Eq. (9). Eq. (1), however, explains only real permittivities.

4. Results

P(VDF–TrFE) films 2 μm thick with compositions of 56/44 and 70/30 mol% have been prepared by spin-coating from solution in dimethylformamide using material from Solvay. The annealing was performed at 120°C for 3 h. The first, second and third-order permittivities were measured at a frequency of 1 kHz and an amplitude of 8 V/μm as a function of temperature for poled and unpoled, annealed and unannealed samples.

4.1. Description with the Landau theory

Fig. 3 shows the temperature dependence of the nonlinear dielectric permittivities of poled and unpoled 56/44 mol% P(VDF–TrFE). The experimental results are compared with the Landau theory taking into account the semicrystallinity by the capacitor model (Sections 2.1 and 2.2). The Landau parameters are determined successively as explained in the following. The crystallinity X_c is known from the literature [8]. α is obtained from the temperature dependence of $1/\epsilon_1$ in the paraelectric phase. It shows a linear dependence on temperature. At the Curie temperature of our semicrystalline material the reciprocal first-order permittivity $1/\epsilon_1$ does not vanish as it would be the case for an idealized ferroelectric crystal with a second-order phase transition. Its value depends on the crystallinity of the sample and the permittivity of the amorphous phase ϵ_a , which is in serial to the crystallites. ϵ_a is therefore extracted from ϵ_1 at the

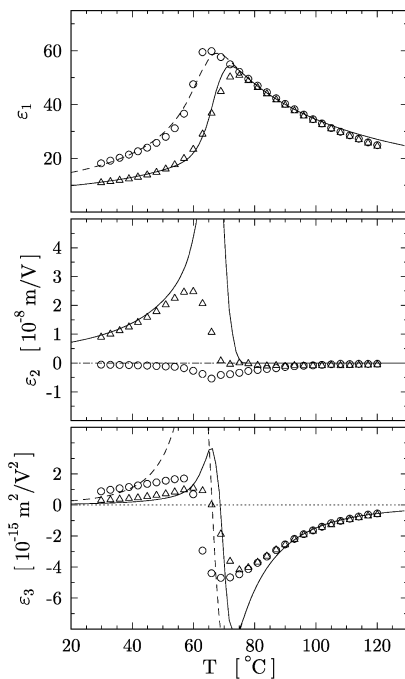


Fig. 3. Nonlinear dielectric permittivities of 56/44 mol% VDF–TrFE copolymer as function of temperature (Δ , —: heating cycle, $X_p = 0.4$; \circ - - -: cooling cycle, $X_p = 0$). The experimental data (symbols) are described by the phenomenological theory (lines) with $\epsilon_a = 8$, $\alpha = (T(^{\circ}\text{C}) - 64) \times 3.3 \times 10^7$ V m/C, $\gamma = -(3.6X_p + 0.4) \times 10^{11}$ V m³/C³, for $T < T_0$ and $\gamma = 1 \times 10^{12}$ V m⁵/C³, for $T > T_0$, $\delta = 2.1 \times 10^{13}$ V m⁹/C⁵. A Gaussian distribution of Curie temperatures of width $\delta_{T_0} = 4^{\circ}\text{C}$ is taken into account.

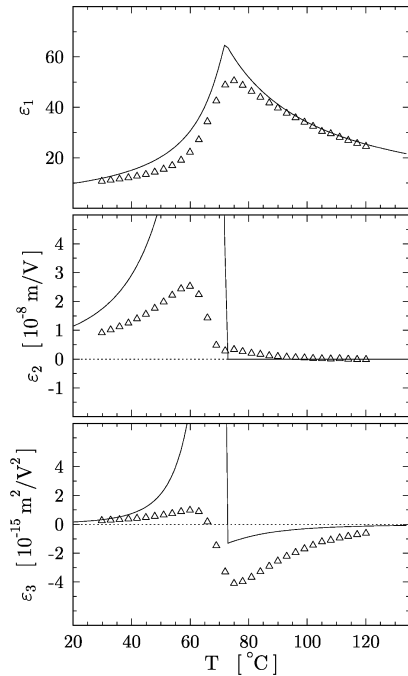


Fig. 4. Nonlinear dielectric permittivities of initially poled 56/44 mol% VDF-TrFE copolymer as function of temperature (heating cycle). The experimental data are described by the microscopical theory with the intra- and interchain interaction energies $J = -1.52$ kJ/mol and $zL = 9.7$ kJ/mol, respectively. The symbols are as in Fig. 3.

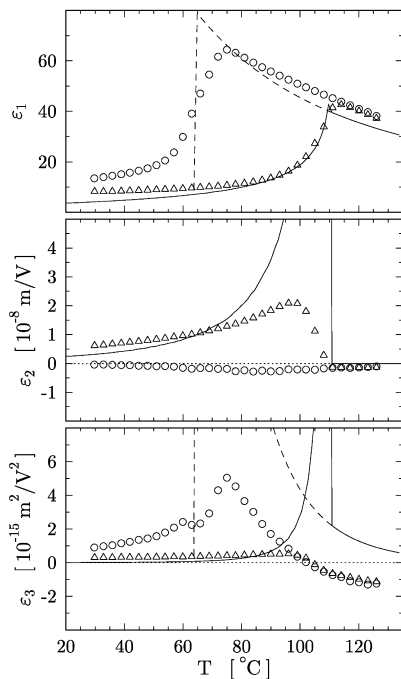


Fig. 5. Nonlinear dielectric permittivities of initially poled 70/30 mol% VDF-TrFE copolymer as function of temperature (heating and cooling cycle). The experimental data are described by the microscopical theory with the intrachain and interchain interaction energies $J = -2.38$ kJ/mol and $zL = 13.1$ kJ/mol, respectively. The symbols are as in Fig. 3.

Curie temperature. ε_3 in the paraelectric phase depends on the parameters already determined and on γ , which can be described by a temperature independent positive value above 90°C . In the ferroelectric phase γ , δ and the poling degree X_p are determined from ε_1 and ε_2 . In this temperature range the experimental data are better described by a small negative γ . That means that the sign of γ changes at the phase transition. As an effect of domain wall motion, ε_1 and ε_3 are functions of the poling degree [7]. The experimentally observed shift of the phase transition temperature with the poling degree is described by the dependence of γ on the poling degree together with a Gaussian distribution of Curie temperatures.

The measured temperature dependencies of the linear, second- and third-order permittivities are not completely described by the phenomenological description. Near the phase transition, the calculated values are higher than the experimental data. In addition, the temperature dependence of the third-order permittivity in the unpoled state is not described satisfactorily. Using more sophisticated functions for the temperature dependence of the Landau parameters, in particular for γ at the phase transition, one could derive theoretical curves that would fit better with the experimental data. However, this would introduce a set of additional parameters and exceed the scope of a phenomenological description. At this point microscopical models have to be studied. A first approach is the theory of Odajima.

4.2. Description with the Odajima theory

The effects of domain wall motion are not included in Odajima's theory. Therefore, we consider only poled material. X_c , ε_a and X_p are assumed to be the same as for the phenomenological description. The mean dipole moment μ and the dipole density N are known. The only fit parameters are the intrachain interaction energy J and the Curie temperature T_0 . The interchain interaction energy L is then evaluated from J and T_0 . J determines the order of phase transition, the width of the thermal hysteresis and the sign of the third-order permittivity in the paraelectric phase. As shown in Figs. 4 and 5, Odajima's theory allows to describe both the first and the second-order phase transition simply by a change of the intrachain interaction energy J . Taking into account that the permittivities of the first, second and third-order of the theoretical calculation are determined only by the same parameter J , the orders of magnitude and the signs of the permittivities are described well. However, the quantitative temperature dependence of the second- and third-order permittivity is not explained well by the theory. This is, however, not very surprising when the approximations in Odajima's theory are considered. The dipoles along a P(VDF-TrFE) chain can actually rotate in steps of 120° [13], i.e. they have three stable states; the Ising model describes a two-state model, however. Furthermore, the dipolar moments of the VDF

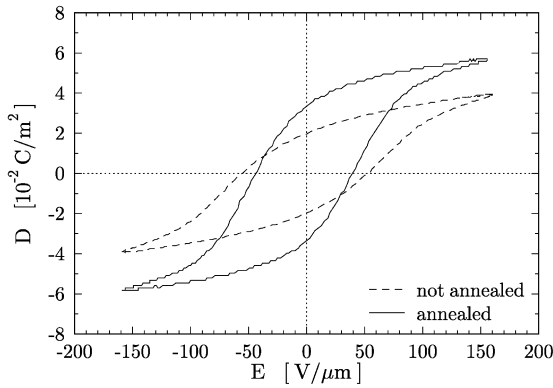


Fig. 6. Hysteresis loops of the dielectric displacement D as a function of the electric field E for an unannealed and an annealed 56/44 mol% VDF–TrFE copolymer sample.

and the TrFE monomers, which differ by a factor of two, are approximated by an average value in the theory.

For a comparison of the Odajima theory with the phenomenological description, the temperature dependence of the Landau parameters can be evaluated from the Odajima model [11]. It yields a negative parameter γ for the 70/30 mol% VDF–TrFE copolymer. For the 56/44 mol% VDF–TrFE copolymer γ changes its sign near the phase transition temperature from a negative value in the ferroelectric phase to a positive value in the paraelectric phase. This is in agreement with our assumption for γ made in the phenomenological description with the Landau theory.

4.3. Permittivity of annealed and unannealed material

The crystallinity of P(VDF–TrFE) copolymers is increased when a sample is annealed after its preparation by spin-coating [12]. Fig. 6 shows the $D(E)$ hysteresis curves measured on an unannealed and an annealed 56/44 mol% VDF–TrFE copolymer sample. Owing to the higher crystallinity the remanent polarization of the annealed sample is 1.7 times higher than that of the

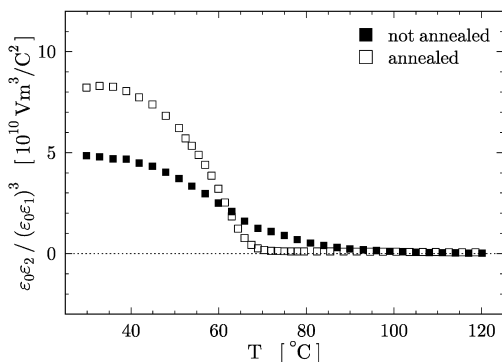


Fig. 7. $\epsilon_0\epsilon_2/(\epsilon_0\epsilon_1)^3$, which is proportional to the remanent polarization P_r , as a function of temperature for an unannealed and an annealed 56/44 mol% VDF–TrFE copolymer sample. The crystallinity of the unannealed film increases during the heating process.

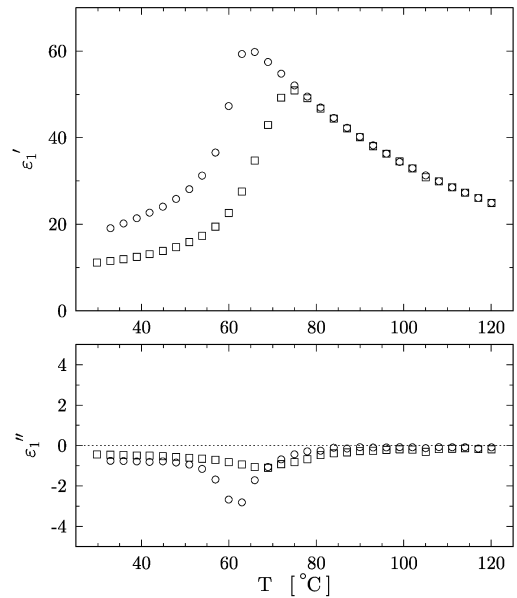


Fig. 8. Temperature dependence of the real part ϵ'_1 and imaginary part ϵ''_1 of the linear permittivity for a poled (\square) and an unpoled (\circ) 56/44 mol% VDF–TrFE copolymer sample measured during a heating cycle. The samples have been annealed before the measurement.

unannealed one. After poling the first and second-order dielectric permittivities of both the samples have been recorded as a function of temperature during heating. In Fig. 7, the quotient $\epsilon_0\epsilon_2/(\epsilon_0\epsilon_1)^3$ shows the decrease of the remanent polarization at the transition to the paraelectric phase for both the annealed and unannealed samples.

The temperature dependence of the linear permittivity of these poled samples are depicted in Figs. 8 and 9 together with the linear permittivity of unpoled samples (annealed and unannealed, respectively). The dielectric properties of the annealed material are clearly influenced by the poling. The linear permittivity of the poled material (Fig. 8) is lower and the transition temperature from the ferroelectric to the paraelectric phase is higher than that of the unpoled material. In contrast, the linear permittivity of unannealed material is not influenced by poling. Fig. 9 shows that there is no difference in the temperature dependence of the linear permittivity of the poled and unpoled samples. The measured second-order permittivity (Fig. 7) proves the remanence of the polarization after the poling process.

This result shows that the change of the dielectric permittivity after poling of an annealed sample cannot be attributed to the different values of the dielectric permittivity in parallel with and perpendicular to the polarization [8], as such a difference would also reduce the dielectric constant of unannealed films after poling. However, the findings can be explained if the difference of the dielectric constant in the poled and in the unpoled state is due to a contribution of domain wall motion [8]. The crystallites of an unpoled annealed sample fall into domains (typically two domains per crystallite [14]). The crystallites become monodomain after poling and the domain wall contribution to the dielectric

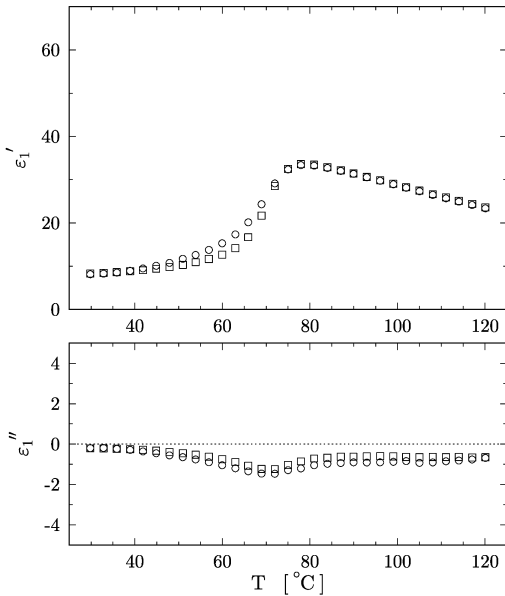


Fig. 9. Temperature dependence of the real part ϵ_1' and imaginary part ϵ_1'' of the linear permittivity for a poled (\square) and an unpoled (\circ) 56/44 mol% VDF-TrFE copolymer sample measured during a heating cycle. The samples were unannealed before the measurement.

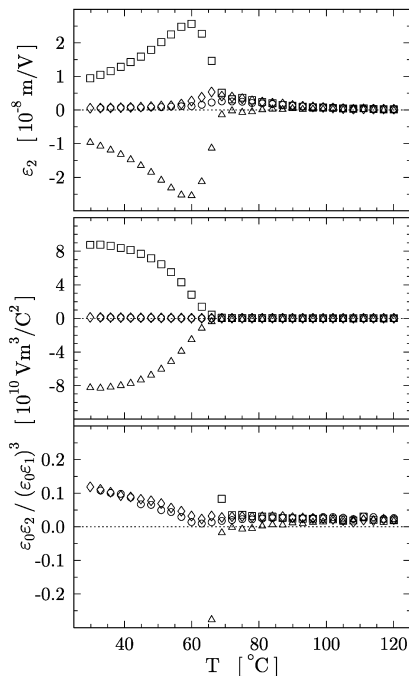


Fig. 10. Second-order nonlinear dielectric permittivity ϵ_2 (real part) of sample A (56/44 mol% VDF-TrFE copolymer annealed directly after preparation) and quotient $\epsilon_0\epsilon_2/(\epsilon_0\epsilon_1)^3$ as a function of temperature. In the lower diagram the vertical axis is spread. The sample poled at room temperature in the positive direction (\square); in the negative direction (Δ); and the unpoled sample (\circ) measured during the heating cycle. The sample poled at room temperature in positive direction (\diamond) measured during the cooling cycle.

constant vanishes. In unannealed samples, the crystallites are smaller (about half the size). For these small crystallites, the formation of domain walls is unfavourable and they are in a monodomain state. Thus no domain wall effects contribute to the dielectric permittivity; it is the same for the poled and for the unpoled case. This explanation is in agreement with X-ray investigations on 73/27 mol% VDF-TrFE copolymer samples with different crystallite sizes prepared by annealing at different temperatures [15].

4.4. Persistent non-switchable polarization in samples poled before annealing

We compared the second-order permittivity of two 56/44 mol% VDF-TrFE copolymer samples. Sample A has been annealed directly after its deposition from solution while sample B was first poled and then annealed.

Fig. 10 shows the temperature dependence of the second-order permittivity of the annealed sample (Sample A) in the unpoled state and in the poled state for two opposite poling directions. In the paraelectric phase ϵ_2 vanishes. In the ferroelectric phase it depends on the poling direction and is zero for the unpoled sample. In Fig. 10, the quotient $\epsilon_0\epsilon_2/(\epsilon_0\epsilon_1)^3$, which is proportional to P_r is also depicted. For the unpoled sample the polarization in the ferroelectric phase is not completely zero but reaches a small value more than two orders of magnitude below the remanent polarization of poled samples. This asymmetry might be due to the slightly different properties of the surfaces of the sample spin-coated on a glass substrate.

Sample B is poled in the positive direction before annealing. After the annealing process the sample is poled and the second-order permittivity is measured. This is depicted in Fig. 11 for the unpoled state and for two different poling directions. Compared with sample A, the temperature dependence is significantly different. Near the Curie temperature and in the paraelectric phase, ϵ_2 occupies positive values instead of being zero like in the case of sample A. The quotient $\epsilon_0\epsilon_2/(\epsilon_0\epsilon_1)^3$ depicted in Fig. 11 indicates a small positive polarization that remains stable in the paraelectric phase. It has the same direction as the polarization of the sample before the annealing. Poling of the annealed sample in the opposite direction does not change this permanent polarization.

During the annealing process the crystallites grow mainly in the direction of the copolymer chains [15]. From the poling experiments on unannealed and annealed material two conclusions can be drawn. The chain links that are built in a crystallite during the first annealing show a preferential dipolar orientation in the direction of its polarization, i.e. in poled material polarization persists in an amorphous interphase near the surface of the crystallites [16–18]. Furthermore, a part of the dipolar chain links built into the crystallites during the first annealing cycle cannot be switched by an electric field. The non-switchable chain

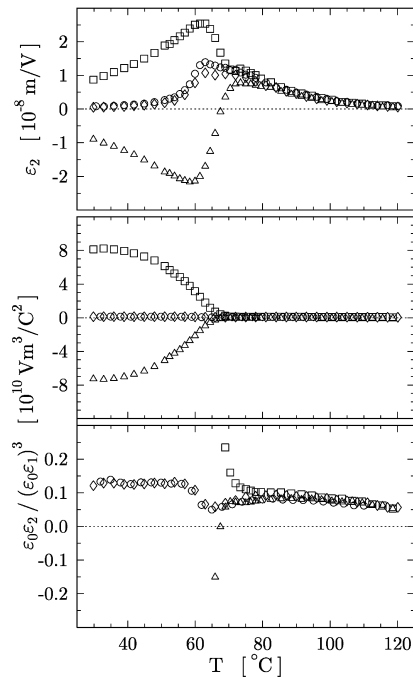


Fig. 11. Second-order permittivity ε_2 of sample B (56/44 mol% VDF–TrFE copolymer poled before the first annealing) and quotient $\varepsilon_0\varepsilon_2/(\varepsilon_0\varepsilon_1)^3$ as a function of temperature. In the lower diagram the vertical axis is spread. The symbols are as in Fig. 10.

links form an intermediate phase between the crystalline and the amorphous phase.

5. Conclusion

The investigation of the nonlinear dielectric permittivities of P(VDF–TrFE) copolymers allows a significant comparison of the experimental data with the theoretical models. The phase transition from the ferroelectric to the paraelectric phase of the crystalline part was described by both the phenomenological Landau and the microscopical Odajima

theory. The semicrystalline structure was taken into account using a capacitor model. A comparison of the linear and second-order permittivity of poled and unpoled unannealed samples shows that the poling degree dependence of the linear permittivity of annealed samples is attributed to domain wall effects. The measurement of the second order dielectric permittivity provides a very sensitive method for the investigation of polarization. Even a very small, fixed and temperature independent polarization can be detected. A persistent non-switchable polarization in samples poled has been found before annealing. It may be attributed to fixed dipoles at the border between the annealed crystallites and the amorphous phase.

References

- [1] Furukawa T. *Ferroelectrics* 1990;104:229–40.
- [2] Heiler B, Ploss B. *Ferroelectrics* 1994;156:285–90.
- [3] Ploss B, Ploss B. *J Korean Phys Soc* 1998;32:S1084–6.
- [4] Ikeda J, Kominami H, Koyama K, Wada Y. *J Appl Phys* 1987;62:3339–42.
- [5] Heiler B, Ploss B. *Proceedings of the Eighth International Symposium on Electrets (ISE 8)*, Paris, 1994. p. 662–7.
- [6] Ikeda J, Suzuki H, Koyama K, Wada Y. *Polym J* 1987;19:681–6.
- [7] Ploss B, Ploss B. *IEEE Trans Dielec Elec Instrum* 1998;5:91–5.
- [8] Legrand JF, Lajzerowicz J, Berge B, Delzenne P, Macchi F, Bourgaux-Leonard C, Wicker A, Krüger JK. *Ferroelectrics* 1988; 78:151–8.
- [9] Odajima A. *Ferroelectrics* 1984;57:159–70.
- [10] Lewis ELV, Ward IM. *J Polym Sci: Polym Phys Ed* 1989;27: 1375–88.
- [11] Ploss B, Ploss B. In preparation.
- [12] Tajitsu Y, Ogura H, Chiba A, Furukawa T. *Jpn J Appl Phys* 1987;26:554–60.
- [13] Tashiro K, Tadokoro H, Kobayashi M. *Ferroelectrics* 1981;32: 167–75.
- [14] Legrand JF. *Ferroelectrics* 1989;91:303–17.
- [15] Tashiro K, Tanaka R, Ushitora K, Kobayashi Y. *Ferroelectrics* 1995;171:145–62.
- [16] Hirschinger J, Meurer B, Weill G. *J Phys* 1989;50:583–97.
- [17] Harnischfeger P, Jungnickel B-J. *Polym Adv Technol* 1990;1:171–9.
- [18] Peterlin A. *Colloid Polym Sci* 1987;265:357–82.